CrossMark

Benchmark study of DFT with Eu and Np Mössbauer isomer shifts using second-order Douglas-Kroll-Hess Hamiltonian

Masashi Kaneko[1] (ID) **· Masayuki Watanabe[1] ·
Sunao Miyashita[2] · Satoru Nakashima[2,3]**

Abstract We optimized a mixing ratio of exchange energy between pure DFT and exact Hartree-Fock using TPSS exchange-correlation functional to estimate the accurate coordination bonds in f-block complexes by numerically benchmarking with the experimental data of Mössbauer isomer shifts for ^{151}Eu and ^{237}Np nuclides. Second-order Douglas-Kroll-Hess Hamiltonian with segmented all-electron relativistically contracted basis set was employed to calculate the electron densities at Eu and Np nuclei, i.e. contact densities, for each five complexes for Eu(III) and Np(IV) systems. We compared the root mean square deviation values of their isomer shifts between experiment and calculation by changing the mixing ratio of Hartree-Fock exchange parameter from 0 to 100% at intervals of 10%. As the result, it was indicated that the mixing ratio of 30 and 60% for Eu and Np benchmark systems, respectively, gives the smallest deviation values. Mulliken's spin population analysis indicated that the covalency in the metal-ligand bonds for both Eu and Np complexes decreases with increasing the Hartree-Fock exchange admixture.

Keywords Mössbauer isomer shift · Density functional theory · F-block coordination chemistry · Chemical bonding · Benchmark study

✉ Masashi Kaneko
    kaneko.masashi@jaea.go.jp

[1] Nuclear Science and Engineering Center, Japan Atomic Energy Agency, 2-4, Shirakata, Tokaimura, 319-1195, Japan

[2] Graduate School of Science, Hiroshima University, 1-3-1, Kagamiyama, Higashi-Hiroshima, 739-8526, Japan

[3] Natural Science Center for Basic Research and Development, Hiroshima University, 1-4-2, Kagamiyama, Higashi-Hiroshima, 739-8526, Japan

Springer

1 Introduction

The bonding study between a metal and ligands on f-block metal complexes is required in the field of nuclear science and engineering. It is because the difference in covalency between lanthanide and actinide complexes has been indicated to be an origin of the selective separation of actinides from lanthanides [1]. To understand the detailed separation system is expected to lead to the development of a rational disposal system of high-level radioactive waste generated in a nuclear fuel cycle [2].

Density functional theory (DFT) has been employed as a useful tool to reveal the electronic and bonding properties for f-block complexes [3–6]. We have performed the benchmark study to estimate accurately the covalent interaction by combining DFT calculation with Mössbauer isomer shift (δ) for ^{151}Eu and ^{237}Np systems [7–9], because Mössbauer isomer shift is a quantitative indicator of chemical bonding [10]. We have also indicated that the optimization of DFT methods by benchmarking can be applied to the improvement for predicting the separation performance and understanding the separation mechanism between Eu and Am ions [11–13].

The present study aims to validate systematically DFT method to estimate the Mössbauer isomer shifts for ^{151}Eu and ^{237}Np systems by parametrizing exact Hartree-Fock exchange admixture in hybrid DFT calculation using TPSS functional [14] as an extension of our previous works [7]. Although this work is performed based on the numerical point of view, not physical point of view, we expect that this attempt leads to the improvement of exchange-correlation (XC) functional to evaluate the covalency in f-block compounds.

2 Computational details

δ can be formulated as the difference in electron density at nuclear position (ρ_0), i.e. contact density, between absorber and source multiplied by the constant coefficient depending on only Mössbauer nuclides (1) [10]:

$$\delta = \{(4\pi/5)Ze^2R^2(\Delta R/R)\}(\rho_0^{\text{absorber}} - \rho_0^{\text{source}}),\qquad(1)$$

where e is the elementary electric charge, Z and R are the nuclear charge and its radius, respectively, and ΔR is the variation of the nuclear radius from ground state to excited state during Mössbauer transition. We can obtain ρ_0 values by a quantum chemical calculation and connect the theoretical calculation with the Mössbauer isomer shifts [15] as follows:

$$\delta^{\text{exp}} = \alpha(\rho_0^{\text{calc}} - \beta).\qquad(2)$$

The linear relationship between the experimental Mössbauer isomer shifts (δ^{exp}) and the calculated ρ_0 values (ρ_0^{calc}) enables us to evaluate the performance of a computational method by comparing the linearity or the root mean square deviation (RMSD) value between δ^{exp} and δ^{calc} values. The δ^{calc} values can be estimated by using the fitting parameters, α and β, which are obtained by the linear regression between δ^{exp} and ρ_0^{calc}.

All DFT calculations were performed by using ORCA ver. 3.0 [16]. Computation of ρ_0 values for the compounds including heavy atoms, such as lanthanides and actinides, requires relativistic Hamiltonian with all-electron basis set for a Mössbauer atom. In this study, we employed scalar-relativistic second-order Douglas-Kroll-Hess (DKH2) Hamiltonian [17] with a finite nucleus model, considering as a uniformly charged sphere [18].

Table 1 Benchmark complexes for Eu and Np systems

Eu complex	δ^{exp}(Eu)/mm s^{-1}		Np complex	δ^{exp}(Np)/mm s^{-1}	
EuCp$_3$(thf)	−1.77(5)	[4.2K]	Np(COT)$_2$	19.4(5)	[4.2K]
EuCpCl$_2$(thf)$_3$	0.06(5)	[4.2K]	NpCp$_3$(OtBu)	8.6(30)	[4.2K]
EuCp(NCS)$_2$(thf)$_3$	0.14(5)	[4.2K]	NpCp$_4$	7.2(2)	[4.2K]
Eu(acac)$_3$(H$_2$O)$_2$	0.36(4)	[80K]	NpCp$_3$(nBu)	2.7(7)	[4.2K]
EuCl$_3$(phen)$_2$	0.57(2)	[80K]	Np(MeCp)Cl$_3$(thf)$_2$	−3.1(7)	[4.2K]

Spin-orbit coupling effect was invariationally considered by using the Breit-Pauli perturbative method. Segmented all-electron relativistic contracted (SARC) basis sets optimized for DKH2 calculation were assigned to Eu [19] and Np [20] atoms. Triple-zeta valence basis set with one polarization function (TZVP), whose contraction coefficients are optimized for DKH2 Hamiltonian [21], was assigned to the other atoms, as implemented in ORCA program [16]. RI approximation was employed for all self-consistent field (SCF) calculation as Split-RI-J method [22] for pure DFT calculation and RIJCOSX method [23] for hybrid DFT calculation. The grid number and accuracy of SCF calculation were employed with the same setting to our previous work [7].

We have indicated that the difference in the mixing ratio of exact Hartree-Fock exchange energy might determine the reproducibility of Mössbauer isomer shifts [7]. In this work, we optimize the exchange admixture using the strategy that includes one empirical parameter (a) for TPSS functional, which is meta-GGA XC functional not including empirical parameters [14]:

$$E_{XC} = (1 - a)E_X^{TPSS} + aE_X^{exact} + E_C^{TPSS}, \tag{3}$$

where E_{XC}, E_X and E_C denote the energies of exchange-correlation, exchange and correlation between two electrons, respectively. In this calculation, we estimated the contact densities by varying a values from 0.0 to 1.0 at intervals of 0.1.

Each five complexes for Eu and Np systems, in which the experimental Mössbauer isomer shifts and DFT-optimized geometries are available in publications [7], were chosen for the benchmarking shown in Table 1. Five trivalent Eu complexes, [EuCp$_3$(thf)] [24], [EuCpCl$_2$(thf)$_3$] [24], [EuCp(NCS)$_2$(thf)$_3$] [24], [Eu(acac)$_3$(H$_2$O)$_2$] [25] and [EuCl$_3$(phen)$_2$] [26] (Cp$^-$ = cyclopentadienyl, thf = tetrahydrofuran, acac$^-$ = acetylacetonato and phen = 1,10-phenanthroline), whose ^{151}Eu Mössbauer isomer shifts are relative to EuF$_3$ vary from –1.77 to 0.57 mm s^{-1} (Table 1), were employed. Five tetravalent Np complexes, [Np(COT)$_2$] [27], [NpCp$_3$(OtBu)] [28], [NpCp$_4$] [29], [NpCp$_3$(nBu)] [28] and [Np(MeCp)Cl$_3$(thf)$_2$] [28] (COT^{2-} = cyclooctatetraenyl, MeCp$^-$ = methycyclopentadienyl), whose ^{237}Np Mössbauer isomer shifts are relative to NpAl$_2$, were employed. We employed the experimental isomer shifts measured at 4.2 K except for [Eu(acac)$_3$(H$_2$O)$_2$] and [EuCl$_3$(phen)$_2$], which were measured at 80 K. It should be noted that the difference in the measured temperature gives no significant effect when considering the variation of isomer shifts for Eu complexes, because the second-order Doppler shift for ^{151}Eu system is ca. 0.02 mm s^{-1} by the difference between 80 K and 4.2 K [30, 31]. We should note that the use of the DFT-optimized geometries is more unfavorable than that of the X-ray geometries as pointed out by Nemykin and coworkers [32]. Unfortunately, since the experimental geometries were not available for all complexes, we used the procedure that the initial structures were created by referring to the analogous X-ray geometries and optimized in the same DFT condition [7]. In this paper, we do not discuss the coordination structures,

Table 2 Calculated electron densities at Eu nucleus position and linear regression parameters at three different mixing parameters

Eu complex	$\delta^{exp}/$ mm s^{-1}	$a = 0.0$		$a = 0.5$		$a = 1.0$	
		$\rho^{calc}/$ a.u.$^{-3}$	$\delta^{calc}/$ mm s^{-1}	$\rho^{calc}/$ a.u.$^{-3}$	$\delta^{calc}/$ mm s^{-1}	$\rho^{calc}/$ a.u.$^{-3}$	$\delta^{calc}/$ mm s^{-1}
EuCp$_3$(thf)	−1.77(5)	822625.308	−1.291	821767.424	−1.588	820894.614	−1.510
EuCpCl$_2$(thf)$_3$	0.06(5)	822634.080	−0.376	821773.871	−0.084	820899.425	−0.140
EuCp(NCS)$_2$(thf)$_3$	0.14(5)	822634.447	−0.338	821773.539	−0.162	820899.377	−0.154
Eu(acac)$_3$(H$_2$O)$_2$	0.36(4)	822643.478	0.604	821775.727	0.349	820900.694	0.222
EuCl$_3$(phen)$_2$	0.57(2)	822644.994	0.762	821777.856	0.845	820903.223	0.942
Correlation coefficient		0.888		0.968		0.949	
α / mm s^{-1} a.u.^{3}		0.104		0.233		0.285	
β / a.u.		822637.689		821774.232		820899.916	
RMSD / mm s^{-1}		4.548		3.681		4.081	

Table 3 Calculated electron densities at Np nucleus position and linear regression parameters at three different mixing parameters

Np complex	$\delta^{exp}/$ mm s^{-1}	$a = 0.0$		$a = 0.5$		$a = 1.0$	
		$\rho^{calc}/$ a.u.$^{-3}$	$\delta^{calc}/$ mm s^{-1}	$\rho^{calc}/$ a.u.$^{-3}$	$\delta^{calc}/$ mm s^{-1}	$\rho^{calc}/$ a.u.$^{-3}$	$\delta^{calc}/$ mm s^{-1}
Np(COT)$_2$	19.4(5)	20327308.084	13.250	20284194.984	15.257	20241268.493	14.078
NpCp$_3$(OtBu)	8.6(30)	20327395.838	5.519	20284297.972	5.728	20241339.805	6.172
NpCp$_4$	7.2(2)	20327296.565	14.265	20284214.733	13.429	20241269.831	13.929
NpCp$_3$(nBu)	2.7(7)	20327431.248	2.399	20284340.188	1.822	20241378.030	1.934
Np(MeCp)Cl$_3$(thf)$_2$	−3.1(7)	20327465.651	−0.632	20284375.387	−1.435	20241407.318	−1.313
Correlation coefficient		−0.792		−0.869		−0.836	
α / mm s^{-1} a.u.^{3}		−0.088		−0.093		−0.111	
β / a.u.		20327458.477		20284359.876		20241395.474	
RMSD / mm s^{-1}		4.548		3.681		4.081	

because the optimized geometries published in reference [7] were employed for calculating electron densities. Spin ground states were set to septet state and quartet state for Eu(III) and Np(IV) systems, respectively. Mulliken's spin population (ρ_{spin}) [33] was estimated to discuss the strength of covalent interaction between metal and the ligands.

3 Results and discussion

Tables 2 and 3 show the numerical data of the calculated ρ_0 (ρ_0^{calc}) values, calculated δ (δ^{calc}) values, correlation coefficient (R), fitting parameters (α, β) and root mean square deviation (RMSD) values for $a = 0.0$, 0.5 and 1.0 for Eu and Np system, respectively.

When focusing on the tendency in the variation between isomer shifts and contact densities, the ρ_0^{calc} values in all methods increase from $EuCp_3(thf)$ to $EuCl_3(phen)_2$ and from $Np(COT)_2$ to $Np(MeCp)Cl_3(thf)_2$, corresponding to approximately the increase in Eu system and decrease in Np system of δ^{exp} values. This increase of ρ_0^{calc} indicates that the complex with covalent interaction, such as metal-carbon bond, has smaller ρ_0^{calc} value than the complex with ionic interaction. The inverse tendency in δ^{exp} between ^{151}Eu and ^{237}Np systems is caused by that the sign of $\Delta R/R$ is positive for ^{151}Eu [34, 35] but negative for ^{237}Np [36]. When comparing the variation of ρ_0^{calc} values from $EuCp_3(thf)$ to $EuCl_3(phen)_2$, the variations are 19.7, 10.4 and 8.6 a.u.$^{-3}$ for $a = 0.0$, 0.5 and 1.0, respectively. The decrease of the variation from $a = 0.0$ to $a = 1.0$ was also observed in Np system. This indicates that pure DFT tends to estimate ρ_0 values to be more sensitive to the change of isomer shifts compared to Hartree-Fock method.

We performed the simple determination of the optimum mixing parameter, which was based on the numerical point of view, not the physical point of view. When focusing on the correlation between δ^{exp} and ρ_0^{calc}, the hybrid DFT calculation with $a = 0.5$ using TPSS functional gives higher correlation and lower RMSD values than $a = 0.0$ and 1.0 systems, as shown in the plots between the calculated and experimental δ values (Figs. 1 and 2), in which δ^{calc} values were estimated by using (2) and fitting parameters. The improvement of the correlation originates in the bonding evaluation of $EuCp_3(thf)$ in Eu system and $NpCp_4$ in Np system. We compared RMSD values in the variation of mixing parameter a in Fig. 3. Interestingly, there were the a values giving the lowest RMSD in 0.0 ∼1.0 range for both systems and its value was different between the Eu and Np benchmarking. The values were observed at 0.3 ∼ 0.4 for Eu system and 0.5 ∼ 0.7 for Np system. The lowering of RMSD originates in the improvement of the tendency between δ^{calc} and δ^{exp} shown in $EuCpCl_2(thf)_3$/ $EuCp(NCS)_2(thf)_2$ and $NpCp_3(OtBu)$ / $NpCp_4$ relations. In the Np system, the inconsistency of this tendency, for example, 8.6 / 7.2 mm s^{-1} for δ^{exp} and 5.7 / 13.4 mm s^{-1} for δ^{calc} when $a = 0.5$, remains to be unknown. This irreproducibility might be improved by the consideration of MP2 correlation energy or long-range correction, although it is not clear in the present stage and should be discussed in future work.

We also tried to calculate $\Delta R/R$ values by using fitting parameter α and the relation of (1), although our benchmark sets include the complexes with only $4f^6$ configuration for ^{151}Eu and only $5f^3$ configuration for ^{237}Np. The estimated values were 0.40×10^{-4} ∼ 1.09×10^{-4} for ^{151}Eu and -0.47×10^{-4} ∼ -0.59×10^{-4} for ^{237}Np in 0.0 ∼ 1.0 range of the mixing parameter a. These values were smaller than the reported values, 4.5×10^{-4}[34] ∼ 12.2×10^{-4} [35] for ^{151}Eu and -3.5×10^{-4} ($= \Delta < R^2 > / < R^2 >$) for ^{237}Np [36]. In the present stage, it is not clear whether the reason of this inconsistency of $\Delta R/R$ values is due to a lack of the complexes with other oxidation states in the benchmark sets or the improvement of the consideration of the relativity at scalar-level included in the present calculation.

Figure 4 shows the variation of Mulliken's spin population, ρ_{spin}, for the Eu and Np atoms by changing mixing parameter a for the selected complexes. The ρ_{spin} values decrease with the increase from 0.0 to 0.6 of a values and do not change in the larger a range in the Eu system. This indicates that pure DFT exchange tends to estimate more strongly the covalent interaction compared to exact exchange. It might lead to the sensitive variation of contact densities to the change of isomer shifts. The degree of variation of the ρ_{spin} values is not so large in the Np system compared to the Eu system, especially for $Np(COT)_2$ and $Np(MeCp)Cl_3(thf)_2$ complexes. This might be a reason why the correlation between δ^{exp} and δ^{calc} values except for $NpCp_4$ was almost the same for $a = 0.0$, 0.5 and 1.0 in Fig. 2, leading to a small reduction of RMSD from maximum to minimum by only 20% for Np system compared to about 60% for Eu system. In both the Eu and Np cases, the ordering

Fig. 1 Eu benchmark plots of isomer shifts between the experiments and the calculations with the mixing parameters $a =$ 0.0 (**a**), 0.5 (**b**) and 1.0 (**c**)

(a) $a = 0.0$
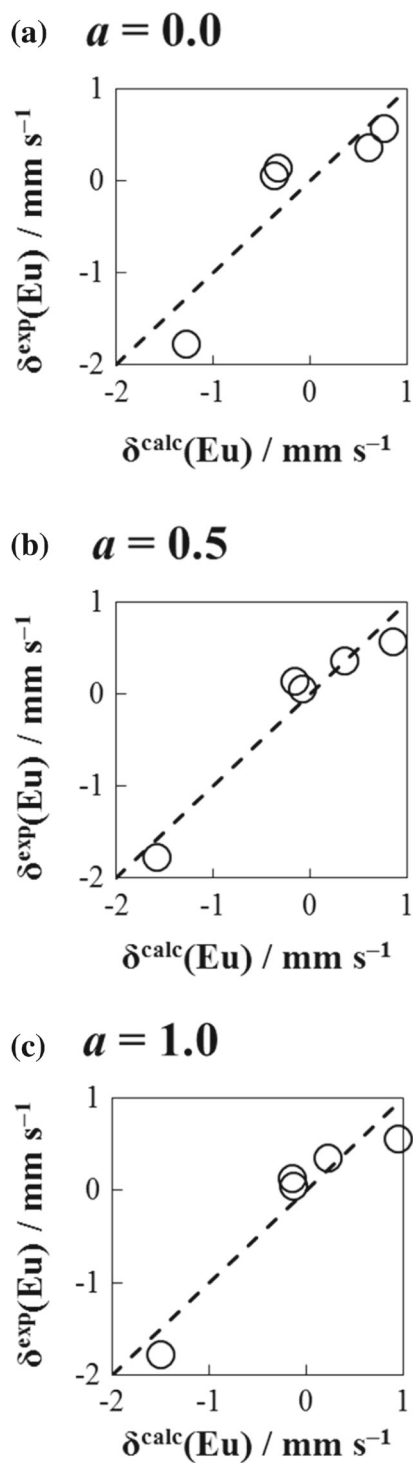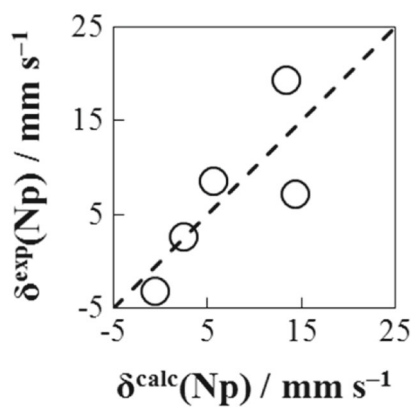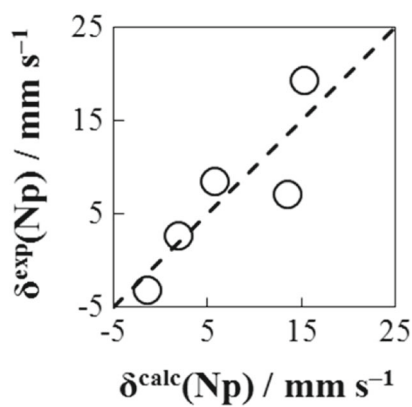
(b) $a = 0.5$

(c) $a = 1.0$

Fig. 2 Np benchmark plots of isomer shifts between the experiments and the calculations with the mixing parameters $a = 0.0$ (**a**), 0.5 (**b**) and 1.0 (**c**)
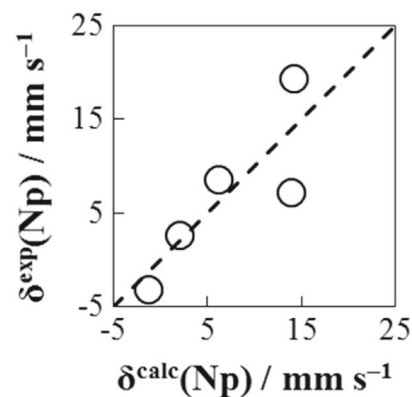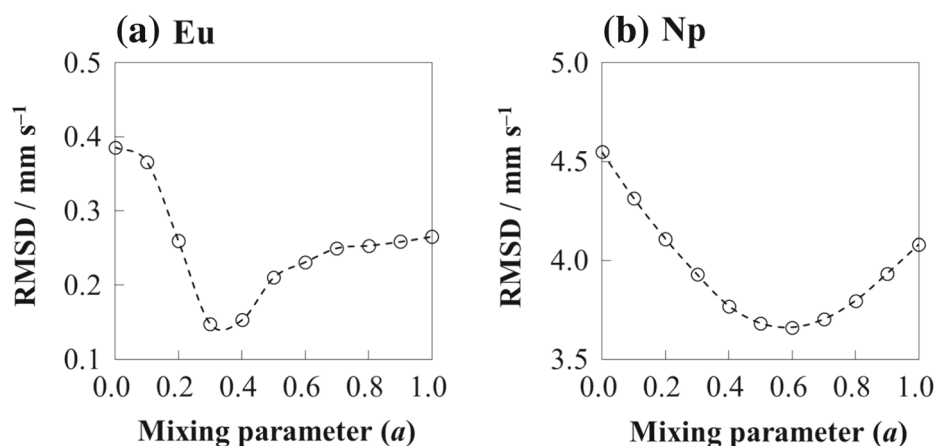

(a) $a = 0.0$

(b) $a = 0.5$

(c) $a = 1.0$

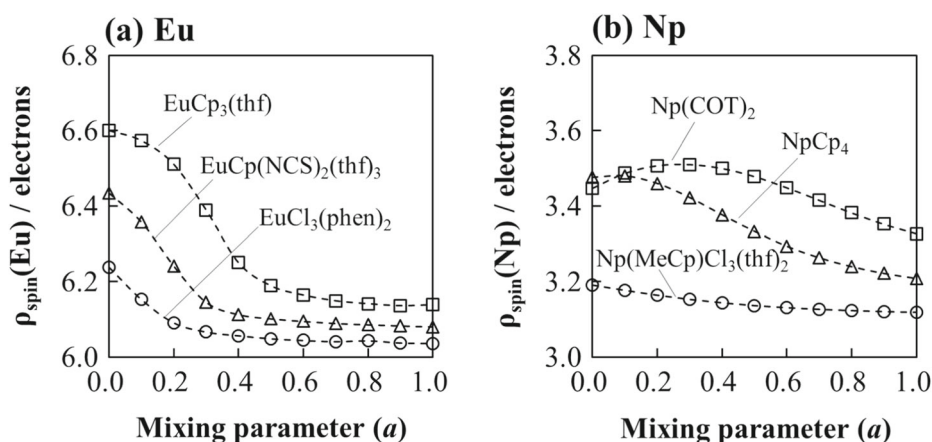**Fig. 3** Comparison of RMSD values with the variation of mixing parameter a for Eu (**a**) and Np (**b**) systems

Fig. 4 Comparison of Mulliken's spin population (ρ_{spin}) with the variation of mixing parameter a for Eu (**a**) and Np (**b**) systems

of ρ_{spin} correlates to that of the corresponding ρ_0 or δ^{exp}, especially in the a range giving a good reproducibility. This correlation was observed in our earlier work [9]. Although the detailed bonding evaluation, including bond overlap population and NBO analyses, is now under study, this results suggest that the isomer shifts change by reflecting the covalent interaction between the metal and the ligands. It is expected that the combination of thus benchmarking with Mössbauer isomer shifts with the quantitative bonding analyses improves the understanding of the coordination bonds in f-block complexes.

4 Conclusion

In summary, we applied scalar-relativistic DFT calculations with DKH2 to the benchmarking with [151]Eu and [237]Np Mössbauer isomer shifts. Varying the mixing ratio of exchange

energy between pure-DFT using TPSS functional and exact Hartree-Fock, we determined the suitable mixing ratio of Hartree-Fock exchange in the hybrid DFT calculations giving the good reproducibility for isomer shifts. The mixing ratio was $30 \sim 40\%$ for Eu complexes and $40 \sim 60\%$ for Np complexes by the simple and numerical determination of lowest RMSD values. Mulliken's population analysis indicated that pure-DFT tends to overestimate the covalency in the coordination bonds for the Eu and Np complexes. It might lead to the oversensitivity of contact density to the change of isomer shifts, resulting in the lowering of the correlation between ρ_0^{calc} and δ^{exp} values.

References

1. Nash, K.L.: A review of the basic chemistry and recent developments in trivalent f-elements separations. Solvent Extr. Ion Exch. **11**, 729–768 (1993)
2. Oigawa, H.: Review of ADS and P&T programme in Japan. Proceedings of 13th OECD/NEA Information Exchange Meeting on Actinide and Fission Product Partitioning and Transmutation (IEMPT-13) 37–43 (2015)
3. Kaltsoyannis, N.: Recent developments in computational actinide chemistry. Chem. Soc. Rev. **32**, 9–16 (2003)
4. Schreckenbach, G., Shamov, G.A.: Theoretical actinide molecular science. Acc. Chem. Res. **43**, 19–29 (2010)
5. Platas-Iglesias, C., Roca-Sabio, A., Regueiro-Figueroa, M., Esteban-Gomez, D., de Blas, A., Rodríguez-Blas, T.: Applications of density functional theory (DFT) to investigate the structural, spectroscopic and magnetic properties of lanthanide (III) complexes. Curr. Inorg. Chem. **1**, 91–116 (2011)
6. Wang, D., van Gunsteren, W.F., Chai, Z.: Recent advances in computational actinoid chemistry. Chem. Soc. Rev. **41**, 5836–5865 (2012)
7. Kaneko, M., Miyashita, S., Nakashima, S.: Benchmark study of Mössbauer isomer shifts of Eu and Np complexes by relativistic DFT calculations for understanding the bonding nature of f-block compounds. Dalton Trans. **44**, 8080–8088 (2015)
8. Kaneko, M., Miyashita, S., Nakashima, S.: Computational study on Mössbauer isomer shifts of some organic-neptunium (IV) complexes. Croat. Chem. Acta. **88**, 347–353 (2016)
9. Kaneko, M., Watanabe, M., Miyashita, S., Nakashima, S.: Bonding study on trivalent europium complexes by combining Mössbauer isomer shifts with density functional calculations. Radioisotopes **66**, 289–300 (2017)
10. Gütlich, P., Link, R., Trautwein, A.: Mössbauer Spectroscopy and Transition Metal Chemistry. Springer, Heidelberg (1978)
11. Kaneko, M., Miyashita, S., Nakashima, S.: Bonding study on the chemical separation of Am(III) from Eu(III) by S-, N-, and O-donor ligands by means of all-electron ZORA-DFT calculation. Inorg. Chem. **54**, 7103–7109 (2015)
12. Kaneko, M., Watanabe, M., Matsumura, T.: The separation mechanism of Am(III) from Eu(III) by diglycolamide and nitrilotriacetamide extraction reagents using DFT calculations. Dalton Trans. **45**, 17530–17537 (2016)
13. Kaneko, M., Watanabe, M., Miyashita, S., Nakashima, S.: Roles of d- and f-orbital electrons in the complexation of Eu(III) and Am(III) ions with alkyldithiophosphinic acid and alkylphosphinic acid using scalar-relativistic DFT calculations. J. Nucl. Radiochem. Sci. **17**, 9–15 (2017)
14. Tao, J., Perdew, J.P., Staroveroc, V.N., Scuseria, G.E.: Climbing the density functional ladder: Nonempirical meta-generalized gradient approximation designed for molecules and solids. Phys. Rev. Lett. **91**, 146401_1-146401_4 (2003)
15. Neese, F., Petrenko, T.: Quantum Chemistry and Mössbauer Spectroscopy. Springer, Heidelberg (2011)
16. Neese, F.: The ORCA program system. WIREs Comput. Mol. Sci. **2**, 73–78 (2012)
17. Nakajima, T., Hirao, K.: The Douglas-Kroll-Hess approach. Chem. Rev. **112**, 385–402 (2012)
18. Visscher, L., Dyall, K.G.: Dirac-fock atomic electronic structure calculations using different nuclear charge distributions. Atom. Data Nucl. Data Tabl. **67**, 207–224 (1997)

19. Pantazis, D.A., Neese, F.: All-electron scalar relativistic basis sets for the lanthanides. J. Chem. Theory Comput. **5**, 2229–2238 (2009)
20. Pantazis, D.A., Neese, F.: All-electron scalar relativistic basis sets for the actinides. J. Chem. Theory Comput. **7**, 677–684 (2011)
21. Pantazis, D.A., Chen, X., Landis, C.R., Neese, F.: All-electron scalar relativistic basis sets for third-row transition metal atoms. J. Chem. Theory Comput. **4**, 908–919 (2008)
22. Neese, F.: An improvement of the resolution of the identity approximation for the formation of the Coulomb matrix. J. Comput. Chem. **35**, 1740–1747 (2003)
23. Neese, F., Wennmohs, F., Hansen, A., Becker, U.: Efficient, approximate and parallel Hartree-Fock and hybrid DFT calculations. A 'chain-of-spheres' algorithm for the Hartree-Fock exchange. Chem. Phys. **356**, 98–109 (2009)
24. Depaoli, G., Russo, U., Valle, G., Grandjean, F., Williams, A.F., Long, G.J.: 4f orbital covalence in $(\eta^5\text{-}C_5H_5)_3Eu(THF)$ as revealed by europium-151 Mössbauer spectroscopy. J. Am. Chem. Soc. **116**, 5999–6000 (1994)
25. Katada, M., Ishiyama, T., Kawata, S., Kondo, M., Kitagawa, S.: ^{151}Eu-Mössbauer spectroscopic studies of europium complexes. Conference proceesings Vol. 50 "ICAME-95", ed. ortalli, I., SIF, Bologna (1996)
26. Burger, K., Nemes-Vetéssy, Z., Vértes, A., Kuzmann, E., Suba, M., Kiss, J.T., Ebel, H., Ebel, M.: Mössbauer study of mixed-ligand complexes of europium(III). Struct. Chem. **1**, 251–258 (1990)
27. Karraker, D.G., Stone, J.A.: Bis(cyclooctatetraenyl)neptunium(III) and –plutonium(III) compounds. J. Am. Chem. Soc **96**, 6885–6888 (1974)
28. Karakker, D.G., Stone, J.A.: Covalency of neptunium(IV) tris(cyclopentadienyl) compounds from Mössbauer spectra. Inorg. Chem. **18**, 2205–2207 (1979)
29. Karakker, D.G., Stone, J.A.: Mössbauer and magnetic suspectibility studies of uranium(III), uranium(IV), neptunium(III), and neptunium(IV) compounds with the cyclopentadiene ion. Inorg. Chem. **11**, 1742–1746 (1972)
30. Deeney, F.A., Delaney, J.A., Ruddy, V.P.: Non-linearity and hysteresis effects in the variation with temperature of the isomer shift in Eu_2O_3. Phys. Lett. A **27**, 571–572 (1968)
31. Wortmann, G., Blumenröder, S., Freimuth, A., Riegel, D.: ^{151}Eu-Mössbauer study of the high-T_c superconductor $EuBa_2Cu_3O_{7-x}$. Phys. Lett. A **126**, 434–438 (1988)
32. Nemykin, V.N., Hadt, R.G.: Influence of Hartree-Fock exchange on the calculated Mössbauer isomer shifts and quadruple splittings in ferrocene derivatives using density functional theory. Inorg. Chem. **45**, 8297–8307 (2006)
33. Mulliken, R.S.: Electronic population analysis on LCAO–MO molecular wave functions I. J. Chem. Phys. **23**, 1833–1840 (1955)
34. Gerth, G., Kienle, P., Luchner, K.: Chemical effects on the isomer shift in ^{151}Eu. Phys. Lett. **27A**, 557–558 (1968)
35. Brix, P., Hüfner, S., Kienle, P., Quitmann, D.: Isomer shift on Eu^{151}. Phys. Lett **13**, 140–142 (1964)
36. Greenwood, N.N., Gibb, T.C.: Mössbauer Spectroscopy, pp. 596-604. Chapman and Hall Ltd., London (1971)